Available online at www.sciencedirect.com
ScienceDirect
Journal of Environmental Sciences 21(2009) 985–990
JOURNAL OF ENVIRONMENTAL SCIENCES
ISSN 1001-0742
CN 11-2629/X
www.jesc.ac.cn

In situ adsorption-catalysis system for the removal of *o*-xylene over an activated carbon supported Pd catalyst

HUANG Shaoyong, ZHANG Changbin, HE Hong*

Research Center for Eco-Environmental Sciences, Chinese Academy of Sciences, Beijing 100085, China. E-mail: syhuang@rcees.ac.cn

Received 28 May 2008; revised 04 July 2008; accepted 21 August 2009

Abstract

An activated carbon (AC) supported Pd catalyst was used to develop a highly efficient *in situ* adsorption-catalysis system for the removal of low concentrations of *o*-xylene. In this study, three kinds of Pd/AC catalysts were prepared and tested to investigate the synergistic efficiency between adsorption and catalysis for *o*-xylene removal. The Pd/AC catalyst was first used as an adsorbent to concentrate dilute *o*-xylene at low temperature. After saturated adsorption, the adsorbed *o*-xylene was oxidized to CO_2 and H_2O by raising the temperature of the catalyst bed. The results showed that more than 99% of the adsorbed *o*-xylene was completely oxidized to CO_2 over a 5% Pd/AC catalyst at 140°C. Brunauer-Emmett-Teller (BET) analysis, scanning electron microscopy (SEM), temperature-programmed desorption (TPD), and temperature-programmed oxidation (TPO) were applied to investigate the physical properties of *o*-xylene adsorption-desorption and the *in situ* adsorption-catalysis activity of the AC support and Pd/AC catalyst. A synergistic relationship between the AC support and the active Pd species for the removal of low concentrations of *o*-xylene was established.

Key words: *in situ* adsorption-catalysis; Pd/AC; volatile organic compounds

DOI: 10.1016/S1001-0742(08)62372-4

Introduction

Volatile organic compounds (VOCs) are a major category of pollutants in indoor and outdoor air, contributing to the formation of photochemical smog and to the destruction of the ozone layer (Finlayson-Pitts and Pitts, 1997). Benzene, toluene, and xylene (BTX) are major VOCs in the environment and of particular concern due to their potentially highly toxic effects on humans (Jones, 1999).

Many techniques have been developed to remove BTX from polluted air, including photocatalytic decomposition (Cao *et al*., 2000; Sun *et al*., 2007; Xie *et al*., 2004). However, the intermediates produced during photocatalytic oxidation occupy the active sites of the catalyst surface, thereby deactivating the catalyst. Some researchers have used plasma to generate reactive species, including energetic electrons and atomic oxygen, to oxidize BTX into CO_2 and H_2O (Delagrange *et al*., 2006; Ogata *et al*., 2003; Van Durme *et al*., 2007), but the high energy consumption required by this process and the formation of undesired byproducts restrict its application. Adsorption is a good choice for the removal of BTX. For example, activated carbon (AC) has been widely employed as an adsorbent to remove VOCs because of its large surface area and its chemical inertness in both acidic and basic media (Auer *et al*., 1998; Cameron *et al*., 1990). However, this technique only sequesters the contaminants in another phase, rather than eliminating them. In another approach, catalytic oxidation was applied to the removal of BTX (Li *et al*., 2005; Pérez-Cadenas *et al*., 2008; Wu *et al*., 2000). In this context, supported Pd catalysts have been studied extensively because of their thermal stability and high activity. The drawback is that although catalytic oxidation converts VOCs into CO_2 and H_2O, the reaction temperature must be maintained, which requires significant energy input. For low-concentration VOCs, an adsorber-incinerator process has been evaluated (Kullavanijaya *et al*., 2000), in which VOCs are first concentrated by adsorption at low temperature until breakthrough occurs. The adsorbent is regenerated by passing a heated inert gas through the bed. The desorbed VOCs are then moved through an incinerator, in which they are converted to harmless compounds by catalytic oxidation. This adsorption-desorption-oxidation process is carried out in two different functional units. Combining the adsorption and oxidation steps into one unit would provide an energy- and cost-effective technique for the removal of low-concentration VOCs. Previous studies compared the removal of dilute toluene (Baek *et al*., 2004) and cyclohexene (Kullavanijaya *et al*., 2002) using adsorption-catalysis systems of $Pd/CeO_2/Al_2O_3$ and Ag/HY, respectively. The results showed that desorption occurred below the working temperature of the catalytic reaction, leading the authors to conclude that the adsorbent and catalyst could not be operated together. However, using a catalyst that exhibits high activity at low temperature

* Corresponding author. E-mail: honghe@rcees.ac.cn

would resolve this problem.

The aim of the present work was to develop a highly efficient *in situ* adsorption-catalysis system based on a Pd/AC catalyst for the removal of *o*-xylene. Brunauer-Emmett-Teller (BET) analysis, scanning electron microscopy (SEM), temperature-programmed desorption (TPD), and temperature-programmed oxidation (TPO) were used to investigate AC structure, *o*-xylene adsorption-desorption, and *in situ* adsorption-catalysis activity of the Pd/AC catalyst. Based on the experimental results, a relationship between AC structure and the adsorption-catalysis efficiency of the Pd/AC catalyst was established.

1 Experimental

1.1 Catalyst preparation

Three AC supports with different surface areas and pore volumes (AC_1, AC_2, and AC_3) purchased from Shanghai Chemical Reagent Co., China were crushed and sieved to 40–60 mesh and then heated at 500°C under a N_2 stream for 3 h to remove adsorbed contaminants. The Pd/AC catalysts were prepared according to the incipient wetness impregnation technique, using AC and an alcohol solution containing the appropriate amounts of $Pd(NO_3)_2$. The samples were dried overnight at room temperature. Prior to the catalytic activity tests, the samples were pre-reduced at 300°C for 1 h in pure H_2 at a flow rate of 30 mL/min.

1.2 Activity tests

Activity tests for the catalytic oxidation of *o*-xylene over Pd/AC were carried out in a continuous-flow fixed-bed reactor under atmospheric pressure. The catalyst was supported on a small plug of glass wool in the middle of a straight-tube Pyrex reactor. To produce *o*-xylene gas, a N_2 stream was bubbled through a saturator filled with liquid *o*-xylene, the concentration of which was controlled by either the flow rate of nitrogen or the temperature of the water bath, which was kept at 0°C. Prior to the activity test, the supported noble metal catalysts were pre-treated at 300°C for 1 h in pure H_2 at a flow rate of 30 mL/min. The reaction feed consisted of 0.08% (*V/V*) *o*-xylene, 20% (*V/V*) O_2, and N_2 as the balance. The flow rate of the gas mixture through the reactor was 50 mL/min. The reactants and products were analyzed on-line using a HP 6890N gas chromatograph (GC) interfaced to a HP 5973N mass-selective detector (Hewlett-Packard, USA) with a HP-5MS capillary column (30 m × 0.25 mm × 0.25 μm) and another GC (GC112A; Shangfen, China) with a carbon molecular sieve column.

1.3 Characterization of the catalyst

BET surface areas were determined in a Quantachrome Autosorb-1C apparatus (Quantachrome Instruments, USA) by physical adsorption measurements using N_2 at a temperature of –196°C. Prior to the measurements, the samples were outgassed at 300°C for 4 h. Images were obtained using a Hitachi S-3000N scanning electron microscope (Hitachi, Japan) with an acceleration voltage of 80 kV.

1.4 Adsorption, desorption, and *o*-xylene oxidation

Adsorption breakthrough curves for *o*-xylene through a fixed-bed reactor were obtained from dynamic measurements at 30°C. The reactor consisted of a 0.6-cm-OD quartz tube with a 0.5-mm-OD thermocouple placed in the center of a bed of 40–60 mesh catalyst particles (0.1 g). The thermocouple measured the temperature and provided feedback to the temperature programmer, which regulated the electrical furnace. A HPR-20 quadruple mass spectrometer (Hiden Analytical, UK) detected products immediately downstream of the reactor as they were desorbed from the catalyst; at the same time, a computer with multiple signals recorded the thermocouple output. The adsorption capacities were determined by the breakthrough curves. The inlet stream for dynamic adsorption was a mixture of 1500 ppmv *o*-xylene in Ar carrier with a flow rate of 50 mL/min. TPD was performed in the same reactor. After saturated adsorption of *o*-xylene at 30°C, the samples were purged under Ar (50 mL/min) flow for 1 h, after which the temperature was increased from 30 to 500°C at a rate of 20°C/min in a flow of Ar, while the temperature and desorption products were recorded. TPO experiments were carried out under the same conditions used for *o*-xylene TPD, except for the presence of 20% (*V/V*) O_2 and the heating ramp of 1°C/min.

2 Results and discussion

2.1 Catalytic activity of Pd/AC catalysts

The activity of the Pd/AC catalysts in the catalytic oxidation of *o*-xylene was tested. The results are shown in Fig. 1. Activities decreased in the following order: Pd/AC_1 > Pd/AC_2 > Pd/AC_3. In the case of the Pd/AC_1 catalyst, *o*-xylene conversion reached 100% at about 190°C and a gas hourly space velocity (GHSV) of 50000 h^{-1}, whereas *o*-xylene conversion using the Pd/AC_2 or Pd/AC_3 catalyst was less than 40% at the same temperature. CO_2 and H_2O

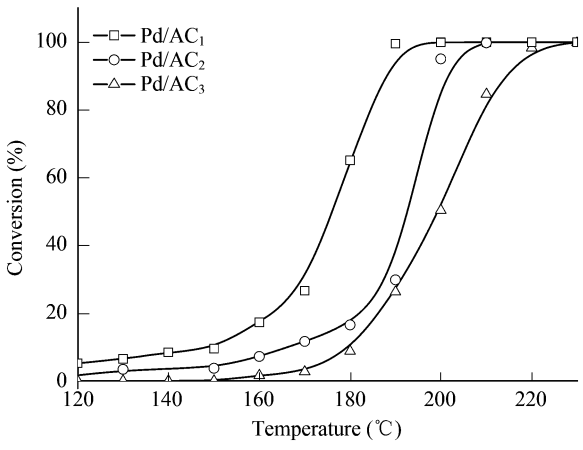

Fig. 1 Catalytic activities of different 1% Pd/AC catalysts for *o*-xylene complete oxidation. Reaction conditions: *o*-xylene 800 ppmv; O_2 20% (*V/V*)/N_2 balance; total flow rate 50 mL/min; GHSV 50000 h^{-1}.

were the only detectable products during the complete oxidation of *o*-xylene.

2.2 Physical characterization of AC supports

To determine why discrepancies in catalytic activity existed among the Pd/AC catalysts, the AC supports were characterized using SEM and BET. As observed in the SEM images of the adoptive AC supports (Fig. 2), the surface morphology of the AC_1 support differed from those of the AC_2 and AC_3 supports. It was previously reported that the differences in the morphologies of AC supports, as observed via electron microscopy, are largely determined by differences in raw materials and manufacturing processes (Auer *et al*., 1998).

The porosity, pore-size distribution, and surface area of the AC support have important effects on adsorptive capacity and activity. To analyze the structural evolution of these supports, the following parameters were investigated: total specific surface area, as calculated by the BET and *t* methods (S_{BET} and S_t); non-microporous specific surface area (S'_t); microporous volume through the *t* method ($V_{mi,t}$); total pore volume (V_{tot}); and average pore size (d). As shown in Table 1, the structures of the three AC supports differed significantly. The S_{BET} and the $V_{mi,t}$ values followed the same order, i.e., $AC_1 < AC_2 < AC_3$. The AC_1 support has the smallest S_{BET} (321.4 m^2/g) and $V_{mi,t}$ (0.074 mL/g), and the AC_3 support has the largest S_{BET} (839.0 m^2/g) and $V_{mi,t}$ (0.310 mL/g). For V_{tot}, the order was $AC_1 \approx AC_2 < AC_3$, and the pore-size (*d*) order was $AC_3 < AC_2 < AC_1$. Thus, it can be clearly seen that AC_3 had more micropores than the other two supports, whereas the AC_1 support had the highest number of mesopores. The large surface area and pore volume of all the three supports contributed to their efficient adsorption of BTX and increased the dispersion of supported active species (Daifullah and Girgis *et al*., 2003; Gaur *et al*., 2006; Zhao *et al*., 2007). However, Pd/AC_1 had the highest activity (Fig. 1), suggesting that the mesopores of the AC support play an important role in *o*-xylene oxidation over the Pd/AC catalyst. Pérez-Cadenas *et al*. (2008) also found that, for *m*-xylene oxidation over a Pd/AC catalyst, the activity of an AC support with micropores was lower than that obtained when using an AC support with mesopores. Micropores have a high adsorption capacity for xylene, which has a minimum kinetic diameter or critical diameter in the range of 0.63–0.74 nm (Roque-Malherbe *et al*., 1995). Accordingly, interactions between large active Pd particles (5–6 nm) located on the mesopores or macropores of the AC support (Aksoylu *et al*., 2001; Kang *et al*., 2002) and the xylene in the micropores are relatively weak and the catalytic activity consequently decreases.

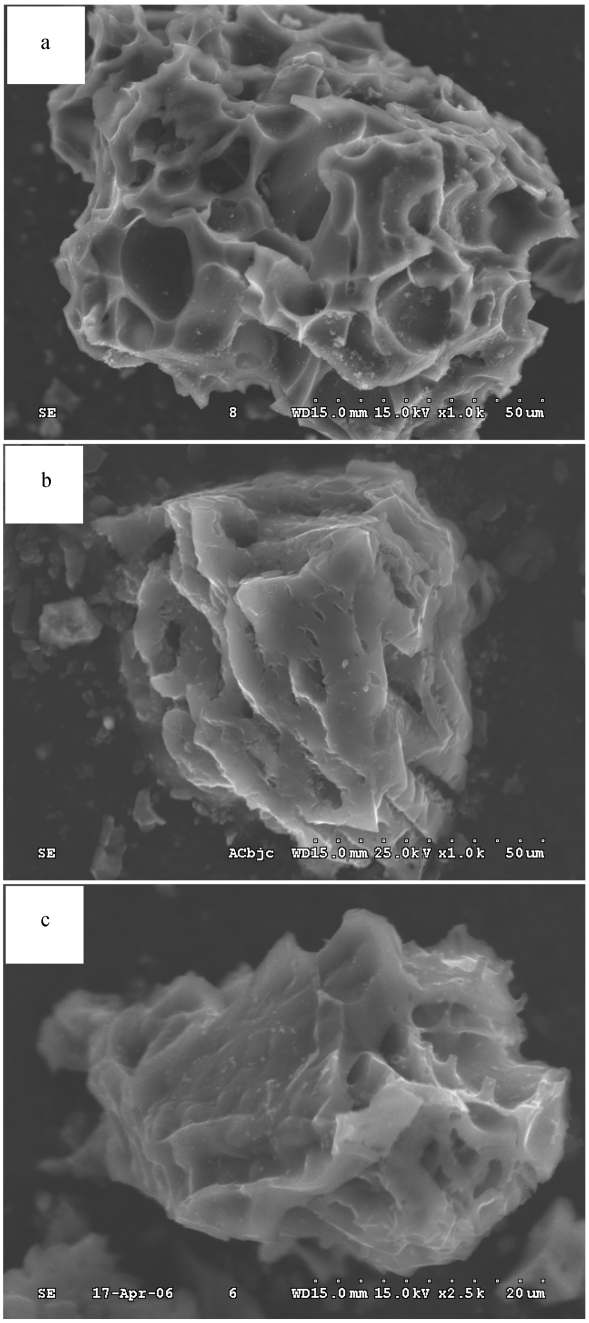

Fig. 2 SEM images of different AC supports. (a) AC_1; (b) AC_2; (c) AC_3.

2.3 *o*-Xylene adsorption and desorption

To better understand the adsorption-catalysis synergism of the Pd/AC catalyst for *o*-xylene removal, *o*-xylene adsorption and desorption on the AC support was investigated by establishing *o*-xylene breakthrough curves and TPD profiles. The *o*-xylene adsorption capacity of the AC support was calculated based on the breakthrough curve (not shown). The saturated adsorption values for *o*-xylene were 116.2, 218.5, and 318.2 mg/g or 3.41, 4.10, 4.28 μmol/m^2 for AC_1, AC_2, and AC_3, respectively, which were linear with the BET values and pore volumes of the AC

Table 1 Porosity characteristic of different AC supports

Sample	S_{BET} (m^2/g)	S_t (m^2/g)	S'_t (m^2/g)	$V_{mi,t}$ (mL/g)	V_{tot} (mL/g)	*d* (nm)
AC_1	321.4	160.2	161.1	0.074	0.3465	4.313
AC_2	501.7	221.2	280.6	0.078	0.3282	2.617
AC_3	839.0	669.7	169.3	0.310	0.5344	2.548

S_{BET}: total specific surface area of the carbons-BET theory; S_t: total specific surface area by *t* method; S'_t: non-microporous specific surface area associated to mesopores by *t* method; $V_{mi,t}$: micropore volume by *t* method; V_{tot}: total pore volume; *d*: average pore size.

supports (Benkhedda *et al*., 2000; Kawasaki *et al*., 2004). Figure 3 shows the *o*-xylene TPD profiles of the three AC supports. It is clear that these profiles differed not only in terms of desorption amounts, but also in the shapes of the curves. *o*-Xylene desorption increased in the order of $AC_1 < AC_2 < AC_3$, consistent with the order of the BET values and the pore volumes of the AC supports (Table 1). Among these TPD profiles, the desorption-peak maximum temperature (T_{max}) of AC_3 was about 200°C compared to about 150°C for AC_1. This difference in *o*-xylene T_{max} values is related to the different adsorption sites for *o*-xylene among the AC supports. Gas molecules adsorbed in mesopores and macropores are more easily desorbed than those in micropores. The BET results showed that, among the three AC supports, AC_1 had the highest concentration of mesopores and thus the lowest T_{max}. It is worth noting that for *o*-xylene, although the AC_1 support had the lowest adsorptive capacity and desorption temperature, the AC_1 supported Pd catalyst had the highest low-temperature catalytic activity (Fig. 1).

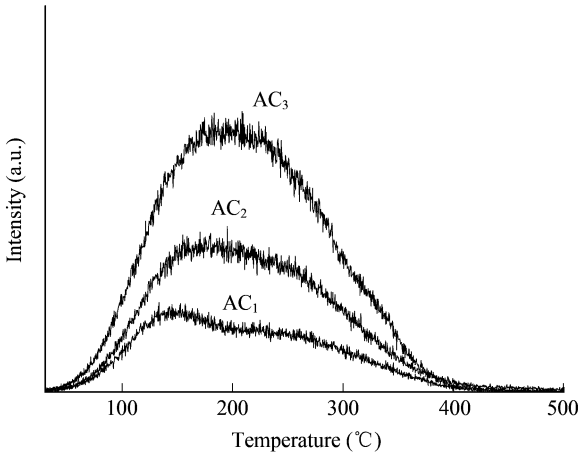

Fig. 3 *o*-Xylene TPD profiles of different AC supports.

The adsorption and desorption of *o*-xylene over 1% Pd/AC catalysts were also studied. The fact that the breakthrough time was the same for *o*-xylene adsorption in the AC_1 support and in the 1% Pd/AC_1 catalyst implies that the adsorptive capacity of the AC_1 support was not changed by 1% Pd loading. As observed in the *o*-xylene TPD profile of the 1% Pd/AC_1 catalyst (Fig. 4), 1% Pd loading on the support had no obvious effect on *o*-xylene adsorption or desorption behavior.

2.4 *o*-Xylene catalytic oxidation

The oxidation of adsorbed *o*-xylene was carried out after saturated adsorption of the compound on the Pd/AC catalysts. TPO of *o*-xylene was achieved within a temperature range of 30–220°C, with a heating ramp of 1°C/min. Figures 5a–5c show the *o*-xylene and CO_2 desorption signals recorded during the oxidation of *o*-xylene over the 1% Pd/AC catalysts. With rising temperature, weak and broad *o*-xylene desorption occurred between 30 and 200°C. Table 2 summarizes the amount of *o*-xylene desorption and the peak maximum temperature of CO_2 production (CO_2 T_{max}) achieved during the oxidation of *o*-xylene over the different Pd/AC catalysts. Compared to the strong *o*-xylene desorption peak of the 1% Pd/AC catalyst tested in the absence of O_2 (Fig. 4), the oxidation of *o*-xylene in the presence of 20% O_2 caused a dramatic decrease in desorption, indicating that the addition of O_2 resulted in complete oxidation of *o*-xylene. The O_2 molecules reacted with the adsorbed *o*-xylene even at low temperatures, which avoided *o*-xylene desorption from the AC support at temperatures below 140°C. The amount of *o*-xylene desorbed followed the same order, i.e., $Pd/AC_1 < Pd/AC_2 < Pd/AC_3$. Based on the catalytic activities of the Pd/AC catalysts, as shown in Fig. 1, it can be concluded that the amount of *o*-xylene desorption is directly, and inversely, influenced by catalytic activity. Moreover, during the oxidation of *o*-xylene, a large CO_2 peak was detected at the final *o*-xylene desorption temperature (about 160–190°C), which confirmed that the disappearance of *o*-xylene desorption was due to oxidation of the compound in the presence of 20% O_2. No obvious byproducts were detected by quadruple mass spectrometry, indicating that the adsorbed *o*-xylene was completely oxidized into CO_2. It should be noted that the oxidation of adsorbed *o*-xylene over Pd/AC catalysts occurs at a lower complete oxidation temperature than that required for *o*-xylene in a continuous-flow fixed bed. This indicates that the adsorption of *o*-xylene from the gas phase to the catalyst surface is the rate-determining step for *o*-xylene oxidation over the Pd/AC catalyst, and that the strong synergistic effect between adsorption and catalysis plays a significant role in the oxidation of the adsorbed *o*-xylene.

With a 5% Pd/AC_1 catalyst, the adsorbed *o*-xylene was completely removed at a temperature about 140°C, and

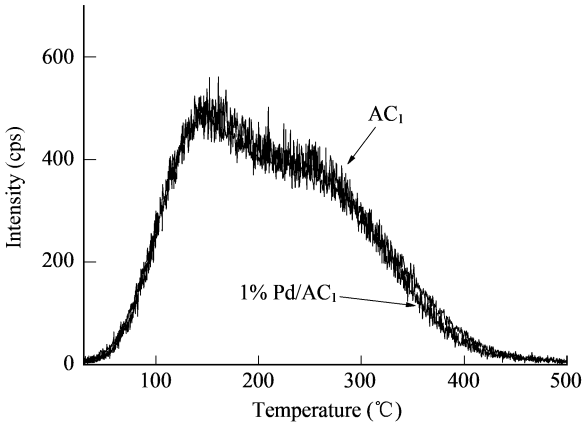

Fig. 4 *o*-Xylene TPD profiles of AC_1 support and 1% Pd/AC_1 catalyst.

Table 2 *o*-Xylene desorption temperature range, *o*-xylene desorption amount and peak maximum temperature of CO_2 during the oxidation of adsorbed *o*-xylene

Sample	Final desorption temperature (°C)	Desorption amount (mg)	Desorption (%)	CO_2 T_{max} (°C)
1% Pd/AC_1	170	0.166	1.43	170
1% Pd/AC_2	190	0.188	0.86	190
1% Pd/AC_3	200	0.645	1.69	200
5% Pd/AC_1	140	0.089	0.76	140

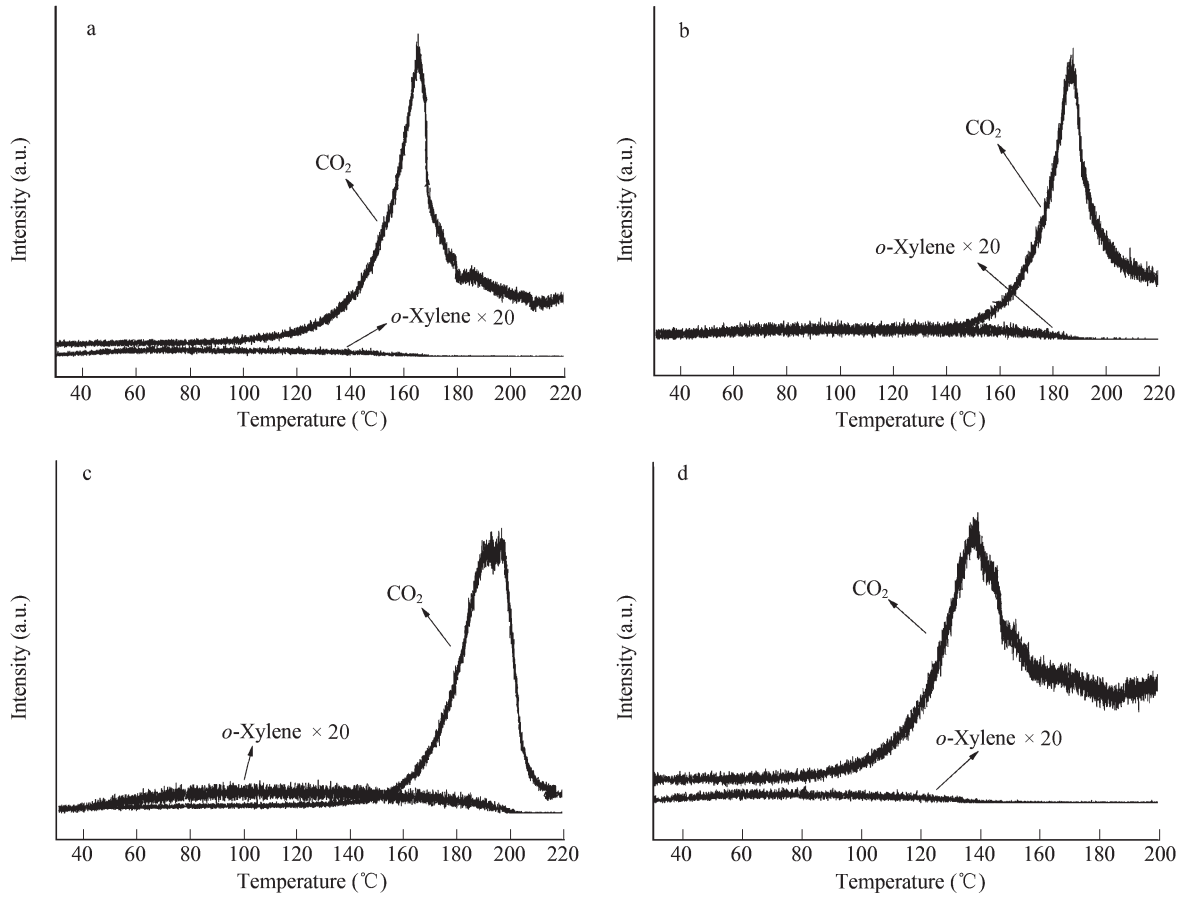

Fig. 5 Oxidation of adsorbed *o*-xylene over different Pd/AC catalysts. (a) 1% Pd/AC_1; (b) 1% Pd/AC_2; (c) 1% Pd/AC_3; (d) 5% Pd/AC_1.

the amount of *o*-xylene desorption was much lower than that measured with the 1% Pd/AC_1 catalyst (Fig. 5d). However, higher Pd loading can also cause the burning of the catalyst during the oxidation of adsorbed *o*-xylene. Taken together, these results provide the evidence that the catalytic activity of Pd/AC determines the amount of *o*-xylene desorption during *o*-xylene catalytic oxidation, and that a strong synergistic effect of adsorption and catalysis is obtained with the Pd/AC catalyst in the removal of low concentrations of *o*-xylene.

3 Conclusions

A highly efficient *in situ* adsorption-catalysis system to remove low concentrations of *o*-xylene using a Pd/AC catalyst was developed. Based on the results of activity tests, BET analysis, SEM, TPD, and TPO, we find that micropores in the AC support play an important role in the adsorption of low concentrations of *o*-xylene, whereas mesopore structure directly influences the activity of the catalyst. The adsorbed *o*-xylene could be completely oxidized into CO_2 and H_2O by raising the temperature of the catalyst bed. Adsorption of *o*-xylene on the catalyst surface was the rate-determining step for *o*-xylene oxidation over the Pd/AC catalyst, and a strong synergistic effect between adsorption and catalysis was found to play a significant role in the oxidation of the adsorbed *o*-xylene. This synergy allowed the complete oxidation of more than 99% of the adsorbed *o*-xylene at a low temperature of 140°C over a 5% Pd/AC catalyst.

Acknowledgments

This work was supported by the National Natural Science Foundation of China (No. 20607029) and the Ministry of Science and Technology of China (No. 2007AA061402).

References

Aksoylu A E, Madalena M, Freitas A, Pereira M F R, Figueiredo J L, 2001. The effects of different activated carbon supports and support modifications on the properties of Pt/AC catalysts. *Carbon*, 39(2): 175–185.

Auer E, Freund A, Pietsch J, Tacke T, 1998. Carbons as supports for industrial precious metal catalysts. *Applied Catalysis A: General*, 173(2): 259–271.

Baek S-W, Kim J-R, Ihm S-K, 2004. Design of dual functional adsorbent/catalyst system for the control of VOC's by using metal-loaded hydrophobic Y-zeolites. *Catalysis Today*, 93-95: 575–581.

Benkhedda J, Jaubert J N, Barth D, Perrin L, Bailly M, 2000. Adsorption isotherms of *m*-xylene on activated carbon: measurements and correlation with different models. *The Journal of Chemical Thermodynamics*, 32(3): 401–411.

Cameron D S, Cooper S J, Dodgson I L, Harrison B, Jenkins J W, 1990. Carbons as supports for precious metal catalysts.

Catalysis Today, 7(2): 113–137.

Cao L, Gao Z, Suib S L, Obee T N, Hay S O, Freihaut J D, 2000. Photocatalytic oxidation of toluene on nanoscale TiO_2 catalysts: Studies of deactivation and regeneration. *Journal of Catalysis*, 196(2): 253–261.

Daifullah A A M, Girgis B S, 2003. Impact of surface characteristics of activated carbon on adsorption of BTEX. *Colloids and Surfaces A: Physicochemical and Engineering Aspects*, 214(1-3): 181–193.

Delagrange S, Pinard L, Tatibouet J M, 2006. Combination of a non-thermal plasma and a catalyst for toluene removal from air: Manganese based oxide catalysts. *Applied Catalysis B: Environmental*, 68(3-4): 92–98.

Finlayson-Pitts B J, Pitts Jr J N, 1997. Tropospheric air pollution: Ozone, airborne toxics, polycyclic aromatichydrocarbons, and particles. *Science*, 276(5315): 1045–1051.

Gaur V, Sharma A, Verma N, 2006. Preparation and characterization of ACF for the adsorption of BTX and SO_2. *Chemical Engineering and Processing*, 45(1): 1–13.

Jones A P, 1999. Indoor air quality and health. *Atmospheric Environment*, 33(28): 4535–4564.

Kang M, Song M W, Kim K L, 2002. Palladium catalysts supported on activated carbon with different textural and surface chemical properties. *Reaction Kinetics and Catalysis Letters*, 76(2): 207–212.

Kawasaki N, Kinoshita H, Oue T, Nakamura T, Tanada S, 2004. Study on adsorption kinetic of aromatic hydrocarbons onto activated carbon in gaseous flow method. *Journal of Colloid and Interface Science*, 275(1): 40–43.

Kullavanijaya E, Cant N W, Trimm D L, 2002. The treatment of binary VOC mixtures by adsorption and oxidation using activated carbon and a palladium catalyst. *Journal of Chemical Technology and Biotechnology*, 77: 473–480.

Kullavanijaya E, Trimm D L, Cant N W, Avelino Corma F V M S M, Jose Luis G F, 2000. Adsocat: Adsorption/catalytic combustion for VOC and odour control. *Studies in Surface Science and Catalysis*, 130(1): 569–574.

Li J J, Xu X Y, Jiang Z, Hao Z P, Hu C, 2005. Nanoporous silica-supported nanometric palladium: Synthesis, characterization, and catalytic deep oxidation of benzene. *Environmental Science and Technology*, 39(5): 1319–1323.

Ogata A, Einaga H, Kabashima H, Futamura S, Kushiyama S, Kim H H, 2003. Effective combination of nonthermal plasma and catalysts for decomposition of benzene in air. *Applied Catalysis B: Environmental*, 46(1): 87–95.

Pérez-Cadenas A F, Morales-Torres S, Kapteijn F, Maldonado-Hodar F J, Carrasco-Marin F, Moreno-Castilla C *et al.*, 2008. Carbon-based monolithic supports for palladium catalysts: The role of the porosity in the gas-phase total combustion of *m*-xylene. *Applied Catalysis B: Environmental*, 77(12): 272–277.

Roque-Malherbe R, Wendelbo R, Mifsud A, Corma A, 1995. Diffusion of aromatic hydrocarbons in H-ZSM-5, H-Beta, and H-MCM-22 zeolites. *Journal of Physical Chemistry*, 99: 14064–14071.

Sun R B, Xi Z G, Chao F H, Zhang W, Zhang H S, Yang D F, 2007. Decomposition of low-concentration gas-phase toluene using plasma-driven photocatalyst reactor. *Atmospheric Environment*, 41(32): 6853–6859.

Van Durme J, Dewulf J, Sysmans W, Leys C, Van Langenhove H, 2007. Efficient toluene abatement in indoor air by a plasma catalytic hybrid system. *Applied Catalysis B: Environmental*, 74(1-2): 161–169.

Wu J C S, Lin Z A, Tsai F M, Pan J W, 2000. Low-temperature complete oxidation of BTX on Pt/activated carbon catalysts. *Catalysis Today*, 63(2-4): 419–426.

Xie C, Xu Z L, Yang Q J, Li N, Zhao D F, Wang D B, Du Y G, 2004. Comparative studies of heterogeneous photocatalytic oxidation of heptane and toluene on pure titania, titania-silica mixed oxides and sulfated titania. *Journal of Molecular Catalysis A: Chemical*, 217(1-2): 193–201.

Zhao Y, Li C H, Yu Z X, Yao K F, Ji S F, Liang J, 2007. Effect of microstructures of Pt catalysts supported on carbon nanotubes (CNTs) and activated carbon (AC) for nitrobenzene hydrogenation. *Materials Chemistry and Physics*, 103(2-3): 225–229.